











# Lysophosphatidylcholine Acyltransferase 1 Deficiency Promotes Pulmonary Emphysema via Apoptosis of Alveolar Epithelial Cells

Takae Tanosaki<sup>1</sup> , Yu Mikami<sup>2</sup> , Hideo Shindou<sup>3,4,8</sup> , Tomoyuki Suzuki<sup>2,3</sup>, Tomomi Hashidate-Yoshida<sup>3</sup>, Keisuke Hosoki<sup>2</sup>, Shizuko Kagawa<sup>1</sup>, Jun Miyata<sup>5</sup> , Hiroki Kabata<sup>1</sup> , Katsunori Masaki<sup>1</sup> , Ryuji Hamamoto<sup>6</sup> , Hidenori Kage<sup>2</sup>, Naoya Miyashita<sup>2</sup>, Kosuke Makita<sup>2</sup>, Hirotaka Matsuzaki<sup>2</sup>, Yusuke Suzuki<sup>7</sup>, Akihisa Mitani<sup>2</sup>, Takahide Nagase<sup>2</sup>, Takao Shimizu<sup>3</sup>  and Koichi Fukunaga<sup>1,8</sup> 

Received 30 November 2021; accepted 7 March 2022

**Abstract**—Chronic obstructive pulmonary disease (COPD) is primarily caused by inhalation of cigarette smoke and is the third leading cause of death worldwide. Pulmonary surfactant, a complex of phospholipids and proteins, plays an essential role in respiration by reducing the surface tension in the alveoli. Lysophosphatidylcholine acyltransferase 1 (LPCAT1) is an enzyme that catalyzes the biosynthesis of surfactant lipids and is expressed in type 2 alveolar epithelial cells. Its dysfunction is suggested to be involved in various lung diseases; however, the relationship between LPCAT1 and COPD remains unclear. To investigate the role of LPCAT1 in the pathology of COPD, we analyzed an elastase-induced emphysema model using *Lpcat1* knockout (KO) mice. In *Lpcat1* KO mice, elastase-induced emphysema was significantly exacerbated with increased apoptotic cells, which was not ameliorated by supplementation with dipalmitoylphosphatidylcholine, which is a major component of the surfactant synthesized by LPCAT1. We subsequently evaluated the effects of cigarette smoking on primary human type 2 alveolar epithelial cells

Takae Tanosaki and Yu Mikami contributed equally to this work.

<sup>1</sup>Division of Pulmonary Medicine, Department of Medicine, Keio University School of Medicine, 35 Shinanomachi, Shinjuku-ku, Tokyo 160-8582, Japan

<sup>2</sup>Department of Respiratory Medicine, Graduate School of Medicine, The University of Tokyo, Tokyo, Japan

<sup>3</sup>Department of Lipid Signaling, National Center for Global Health and Medicine (NCGM), 1-21-1 Toyama, Shinjuku-ku, Tokyo 160-8655, Japan

<sup>4</sup>Department of Lipid Medical Science, Graduate School of Medicine, The University of Tokyo, Tokyo, Japan

<sup>5</sup>Division of Infectious Diseases and Respiratory Medicine, Department of Internal Medicine, National Defense Medical College, Saitama, Japan

<sup>6</sup>Division of Medical AI Research and Development, National Cancer Center Research Institute, Tokyo, Japan

<sup>7</sup>Department of Respiratory Medicine, Kitasato University Kitasato Institute Hospital, Tokyo, Japan

<sup>8</sup>To whom correspondence should be addressed at Division of Pulmonary Medicine, Department of Medicine, Keio University School of Medicine, 35 Shinanomachi, Shinjuku-ku, Tokyo, 160-8582, Japan and Department of Lipid Signaling, National Center for Global Health and Medicine (NCGM), 1-21-1 Toyama, Shinjuku-ku, Tokyo, 160-8655, Japan. Email: hshindou@ri.ncgm.go.jp; kfukunaga@keio.jp

(hAEC2s) and found that cigarette smoke extract (CSE) downregulated the expression of *Lpcat1*. Furthermore, RNA sequencing analysis revealed that the apoptosis pathway was significantly enriched in CSE-treated primary hAEC2s. Finally, we downregulated the expression of *Lpcat1* using small interfering RNA, which resulted in enhanced CSE-induced apoptosis in A549 cells. Taken together, cigarette smoke-induced downregulation of LPCAT1 can promote the exacerbation of pulmonary emphysema by increasing the susceptibility of alveolar epithelial cells to apoptosis, thereby suggesting that *Lpcat1* is a novel therapeutic target for irreversible emphysema.

---

**KEY WORDS:** LPCAT1; emphysema; dipalmitoyl phosphatidylcholine; type 2 alveolar epithelial cell; apoptosis.

## INTRODUCTION

Chronic obstructive pulmonary disease (COPD) is caused by the inhalation of harmful substances, such as cigarette smoke and air pollutants, and has become the third leading cause of death worldwide in recent years [1]. COPD is characterized by airway obstruction and lung emphysema, caused by a range of small airway diseases and airway destruction. In addition, patients with COPD and severe lung emphysema due to alveolar destruction, including alveolar epithelial cell apoptosis, display a rapid decrease in capacity for carbon monoxide diffusion, which results in poor prognosis [2].

Type 2 alveolar epithelial cells (AEC2s) are cube-shaped cells comprising 16% of adult lung parenchymal cells [3]. AEC2s play an important role in the synthesis and secretion of pulmonary surfactants and maintenance of homeostasis in the alveoli through the regulation of fluids and ion transport [4]. In addition, AEC2s differentiate into type 1 alveolar epithelial cells (AEC1s) during lung injury and repair [5]. Moreover, the dysfunction and apoptosis of AEC2s by noxious particles are key features of COPD, particularly the development of lung emphysema [6].

The pulmonary surfactant produced and secreted by AEC2s consists of 90% phospholipids and 10% surfactant-associated proteins [7]. Phospholipids in pulmonary surfactants consist of approximately 80% phosphatidylcholine (PC). In addition, dipalmitoyl-PC (DPPC) is the major component (~30%) of PC in pulmonary surfactants [8]. The key functions of DPPC are to decrease the surface tension for proper alveolar opening and protect lung cells from oxidative stresses. Smoking decreases the amount of PC and surfactant protein (SP)-D in the bronchoalveolar lavage fluid (BALF) [9]. Furthermore, PC including DPPC in the BALF of patients with COPD is lower than

that of healthy individuals, and forced expiratory volume measured during the first second (FEV1) correlates with the amount of PC and DPPC in the BALF [10]. However, although there are reports on the association between SP disorders, such as SP-C [11], SP-D [12], and emphysema, the association between surfactant lipids and emphysema has not been clarified.

PC is biosynthesized by lysophosphatidylcholine acyltransferase (LPCAT) using acyl-coenzyme A and lysophosphatidylcholine as substrates in the remodeling pathway (Lands' cycle) [13–15]. Recently, Chen *et al.* and our group independently discovered LPCAT1 [16, 17] (also known as lysophospholipid acyltransferase 8) [18], which is expressed substantially in the lungs, followed by the spleen and brain [16]. In the lungs, its expression is higher in AEC2s, and it catalyzes the synthesis of DPPC, the major component of pulmonary surfactant [16]. We previously reported that *Lpcat1* knockout (KO) mice produced a similar amount of total PC compared with wild-type (WT) mice; however, the proportion of DPPC was halved [19]. Consequently, *Lpcat1* KO mice displayed a high mortality rate because of respiratory failure [19, 20].

Taken together, we hypothesized that the change in the proportion of DPPC through the dysfunction of LPCAT1 is related to the development of lung emphysema. To test this hypothesis, we compared the severity of lung emphysema induced by porcine pancreatic elastase (PPE) in both WT and *Lpcat1* KO mice.

## MATERIALS AND METHODS

### Mice

Female C57BL/6 N mice were obtained from San'kyo Labo (Tokyo, Japan). All animal experiments and procedures were approved by the Laboratory Animal

Center, the Keio University School of Medicine (Protocol No. 10258), and were performed in accordance with the institutional guidelines. *Lpcat1* KO mice were generated as previously described [19].

### Elastase-Induced Emphysema Mouse Model

Eight-week-old mice (WT and *Lpcat1* KO) were intratracheally injected with 1.5 units of PPE (Elastin Products, Owensville, MO, USA) in 50  $\mu$ L of phosphate-buffered solution (PBS) using a micro-sprayer drug delivery device (Penn-Century, Philadelphia, PA, USA). We used a low dose of PPE (1.5 units) to clarify the differences between *Lpcat1* KO and WT mice. Control mice were age-matched and intratracheally injected with 50  $\mu$ L of PBS. PPE was administered only once, and mice were observed for 6 weeks after administration and then sacrificed. After elastase administration, we observed the mice for up to 6 weeks, considering the possibility that *Lpcat1* deficiency may cause long-term exacerbation of elastase emphysema than what has been reported in previous studies [21, 22]. At least three mice were used in each group.

### Micro-computed Tomography (CT) Imaging

Mice were anesthetized via the inhalation of isoflurane (Pfizer, Tokyo, Japan) and scanned using an X-ray micro-CT system (R\_mCT2; Rigaku, Tokyo, Japan). The system was operated with the following parameters: 90 kV, 160  $\mu$ A, chest CT; respiratory and cardiac reconstruction mode, field of view: 24  $\times$  24 mm (pixel size: 50  $\times$  50  $\mu$ m), and scan time: 4.5 min. For reconstruction, we used the respiratory and cardiac reconstruction mode, which reconstructs lung images only at the diastolic phase of the heart at the end-expiratory period by simultaneously monitoring both respiratory and cardiac motion under X-ray fluoroscopy. To calibrate the CT values, a 15-mL tube of water was scanned and the image was used to set 0 HU for water and 1000 HU for air [23]. We analyzed the micro-CT images using a Lexus 64 workstation (AZE, Tokyo, Japan). Lung parenchyma was arbitrarily defined as a region with X-ray attenuation values between  $-1024$  and  $-450$  HU, and intra- and surrounding extrapulmonary tissues were excluded [23]. Low-attenuation area (LAA) thresholds were arbitrarily set to  $< -780$  HU to calibrate the percentage of LAA to the total lung volume in control mice at  $< 5\%$  [24].

### Morphologic Evaluation of Emphysema

The mice lungs were inflated with 4% paraformaldehyde at a pressure of 25 cmH<sub>2</sub>O for 5 min and fixed in formalin for 24 h at room temperature. Lung tissues were paraffin-embedded, sectioned in the sagittal plane, and stained with hematoxylin and eosin (H & E). Regarding the measurement of the mean linear intercept (Lm), a standard method of air space evaluation [25] was used. In detail, images of five lung lobes were captured using NanoZoomer (Hamamatsu Photonics, Shizuoka, Japan), and 10 fields were randomly selected in each mouse. Two lines were randomly drawn horizontally and vertically on the selected images, and the intersections between the lines and the alveolar walls were counted manually. Lm was calculated by dividing the length of the lines by the number of intersections.

### Terminal Deoxynucleotidyl Transferase dUTP Nick End Labeling (TUNEL) Staining

To evaluate apoptosis, we performed TUNEL staining using a DeadEnd Fluorometric TUNEL System (Promega; Fitchburg, WI, USA) according to the manufacturer's protocol. Apoptotic cell numbers were counted at 1 week following the elastase injection by averaging the five lobe findings for each group, as described previously [26].

### PC Analysis in Lipid Extracts

Lipids were extracted from the BALF using the Bligh and Dyer method [27]. We analyzed the samples using an LCMS8040 and LCMS8050 (Shimadzu Corp., Kyoto, Japan), as described in the Supplementary Materials and Methods.

### Flow Cytometry

Single-cell suspensions and cultured cells were used for flow cytometric analysis. The antibody and staining methods are provided in the Supplementary Materials. Stained cells were run on a Gallios Flow Cytometer (Beckman Coulter, Brea, CA, USA) and analyzed using FlowJo 7.6.2 (Tree Star, Ashland, OR, USA).

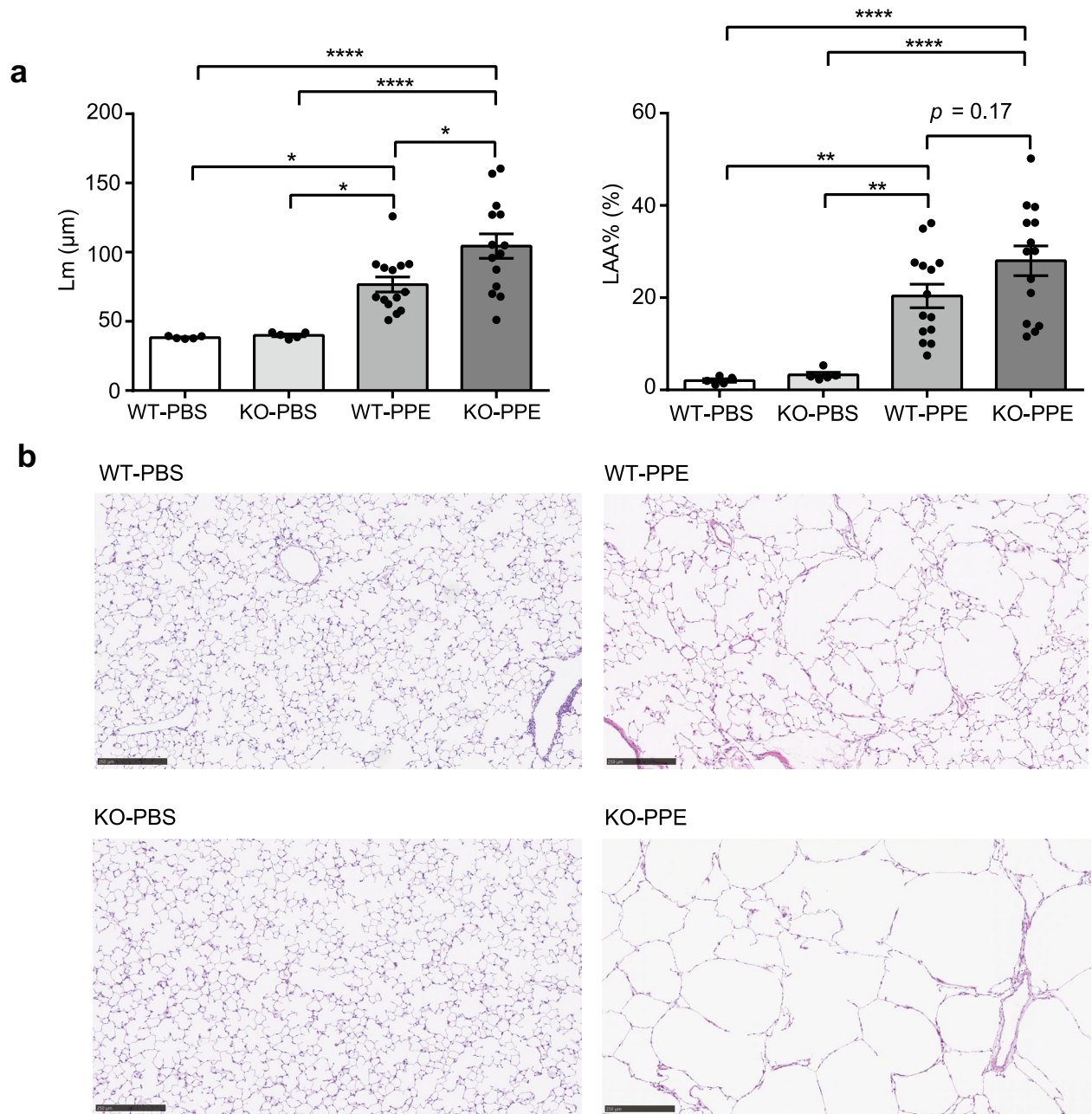


**Fig. 1** *Lpcat1* KO mice have exacerbated PPE-induced emphysema. **(a)** Comparison between WT and *Lpcat1* KO mice 6 weeks after PPE injection. The mean linear intercept (Lm, left) and LAA% (right) are measured as described in the “Materials and Methods” section. **(b)** Representative images of hematoxylin and eosin-stained lung Sects. 6 weeks after PPE or PBS injection in WT or KO mice. Scale bar, 250  $\mu\text{m}$ . Data are presented as mean  $\pm$  standard of mean ( $n=4-14$ ). \*\* $P < 0.01$  (two-way ANOVA with Tukey adjustment). WT: wild type; KO: knockout; PBS: phosphate-buffered solution; PPE: porcine pancreatic elastase; Lm: mean linear intercept; LAA%: low attenuation area %; LPCAT1: Lysophosphatidylcholine acyltransferase 1; ANOVA: analysis of variance.

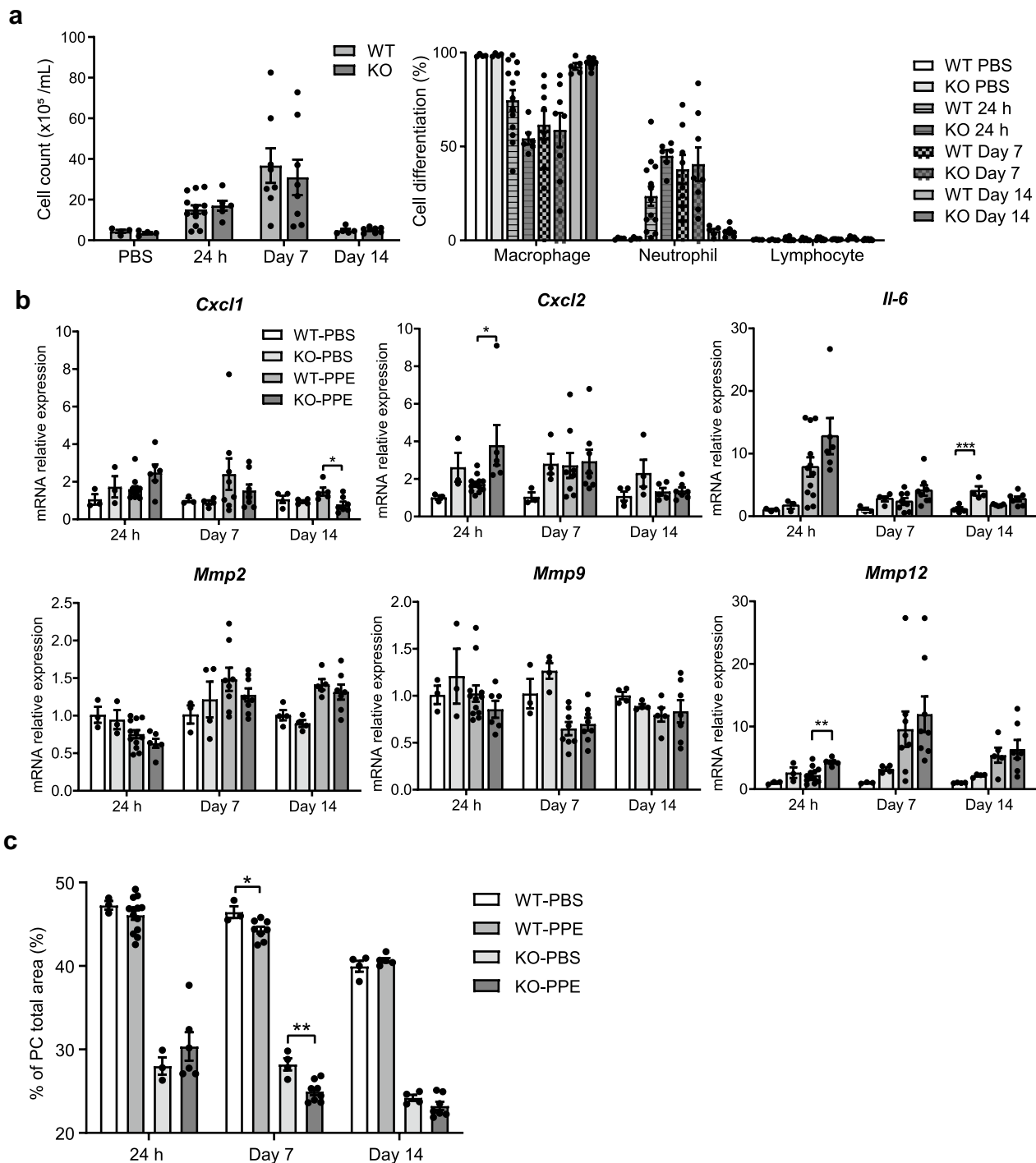
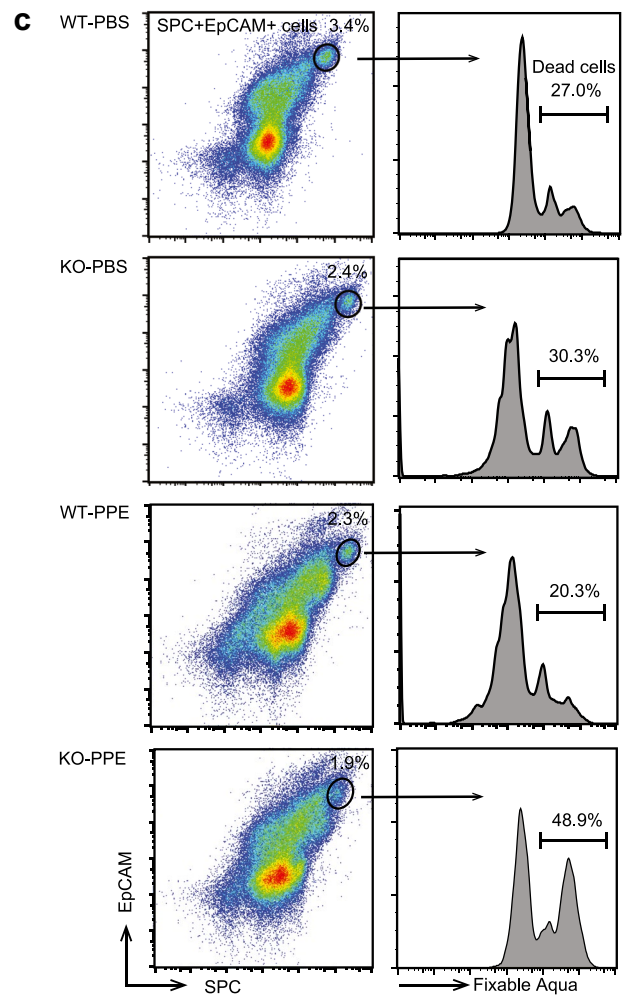
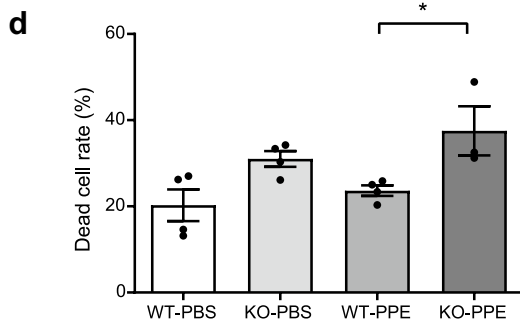
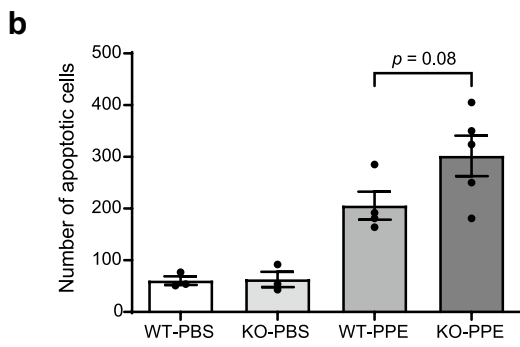
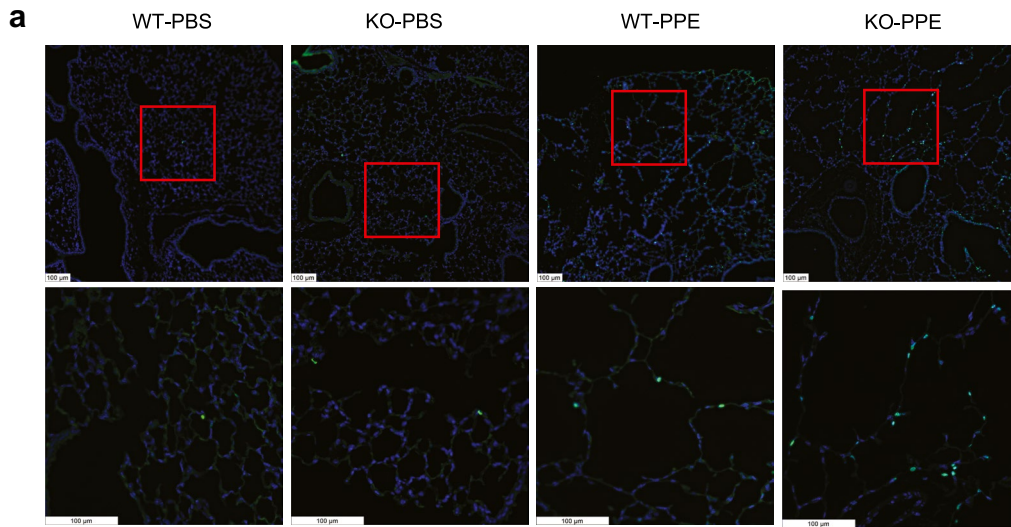


**Fig. 2** Analysis of BALF and whole lung after PPE injection. (a) The number of total cells (left) and the percentage of macrophages, neutrophils, and lymphocytes (right). (b) Relative expression of inflammatory cytokines (*Cxcl1*, *Cxcl2*, *Il6*) and MMPs (*Mmp2*, *Mmp9*, and *Mmp12*) in whole lung tissue at the indicated time points. (c) Percentage of DPPC among total PC content in the BALF. Data are presented as mean  $\pm$  standard of mean ( $n = 3-13$ ). \* $P < 0.05$ , \*\* $P < 0.01$ , and \*\*\* $P < 0.001$  (two-way ANOVA with Bonferroni adjustments). PPE, porcine pancreatic elastase; MMPs: matrix metalloproteinases; DPPC: dipalmitoyl phosphatidylcholine; PC: phosphatidylcholine; BALF: bronchoalveolar lavage fluid; ANOVA: analysis of variance.



◀ **Fig. 3** Increased number of apoptotic cells and mortality of AEC2 in the lungs of *Lpcat1* KO mice 1 week after PPE administration. (a) Representative high power (lower panel) and low power images (upper panel) of TUNEL staining in the lungs, 1 week after PPE administration. Scale bar, 100  $\mu$ m. (b) The number of apoptotic cells. Data are presented as mean  $\pm$  standard error of mean ( $n=3-5$ ). Data are analyzed by two-way ANOVA with Bonferroni adjustments. (c) Representative images of flow cytometric analysis using double staining with SPC and EpCAM (left column) and the histogram of fixable aqua in SPC<sup>+</sup>EpCAM<sup>+</sup> cells (dead AEC2 cells, right column). (d) Dead cell rate in SPC<sup>+</sup>EpCAM<sup>+</sup> cells (AEC2). Data are presented as mean  $\pm$  standard of mean ( $n=3-4$ ). \* $P < 0.05$  (two-way ANOVA with Bonferroni adjustments). PPE, porcine pancreatic elastase; TUNEL: terminal deoxynucleotidyl transferase dUTP nick end labeling; PPE: porcine pancreatic elastase; WT: wild type mice; KO: *Lpcat1* KO mice; AEC2: type 2 alveolar epithelial cells; ANOVA: analysis of variance.

### RNA Sequencing Gene-Expression Analysis in Primary Human Type 2 Alveolar Epithelial Cells (hAEC2s)

Total RNA was extracted from hAEC2s using the RNeasy Mini Kit (Qiagen, Hilden, Germany). We performed library preparation and sequencing using BGI Genomics. All analysis techniques are described in the Supplementary Materials and Methods. All RNA-seq datasets were deposited in the Gene Expression Omnibus database (GSE186359, <https://www.ncbi.nlm.nih.gov/geo/query/acc.cgi?acc=GSE186359>).

### Statistical Analyses

Data are presented as the mean  $\pm$  standard error of the mean and were analyzed using GraphPad Prism 6 (GraphPad Software, San Diego, CA, USA). The Student's *t*-test was performed for comparisons between two groups. We performed the one-way analysis of variance (ANOVA) or two-way ANOVA with Dunnett's multiple comparison tests, Tukey's multiple comparison tests, or Bonferroni's multiple comparison tests for comparisons between three or more groups. Statistical significance was set at  $p < 0.05$ .

## RESULTS

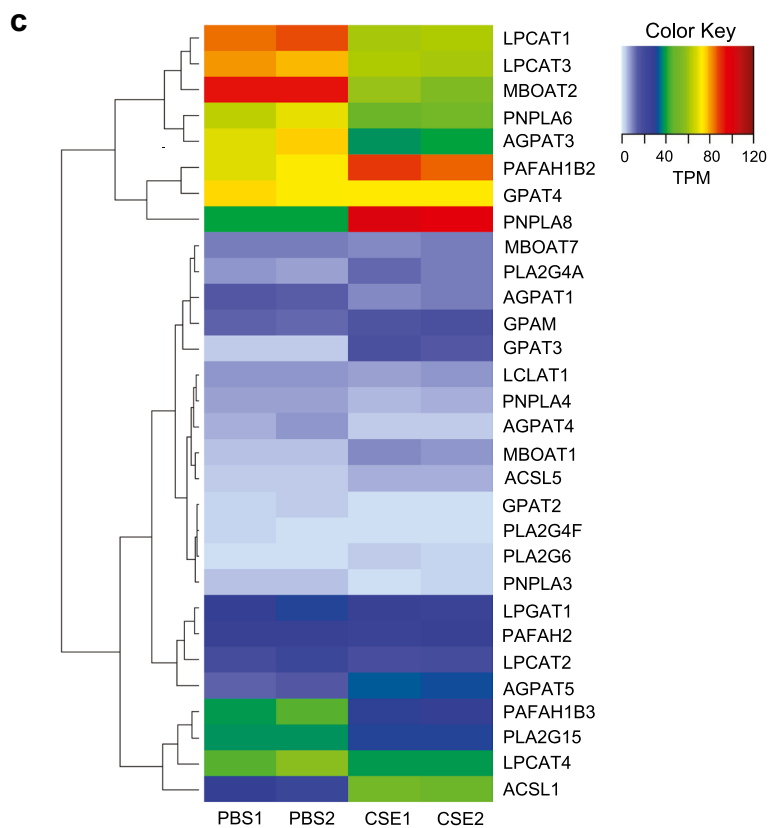
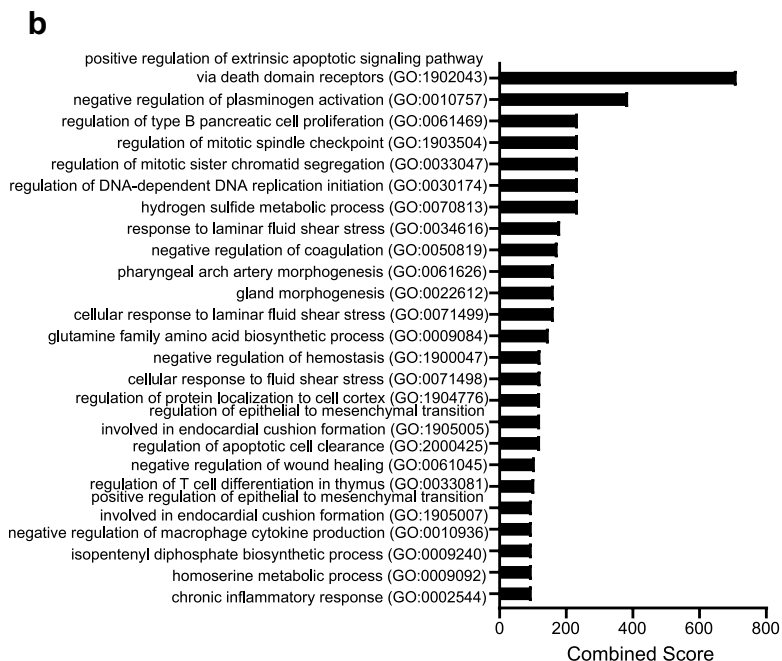
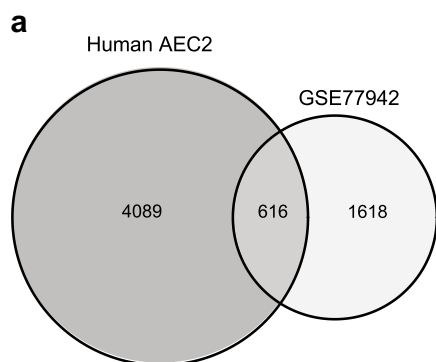
### *Lpcat1* KO Mice Were More Susceptible to PPE-Induced Lung Emphysema

We performed sequential micro-CT at 1, 2, 4, and 6 weeks post-PPE administration for measuring

the LAA percentage (LAA%) to evaluate lung emphysema in mice. We measured the Lm 6 weeks after PPE administration. Micro-CT imaging revealed that PPE-administered mouse lungs displayed a higher LAA% at 1 week after PPE administration than both PBS-treated mouse lungs and mouse lungs before PPE treatment. Furthermore, *Lpcat1* KO mice demonstrated a relatively higher LAA% than WT mice (Supplemental Fig. S1). Six weeks following PPE administration, Lm and LAA% in the PPE-treated group were higher than those in the PBS-treated group. Lm was significantly higher in PPE-treated KO mice than in WT mice (Fig. 1a, left). The LAA% was also higher in PPE-treated KO mice than in WT mice (Fig. 1a, right); however, the increase in LAA% was not statistically significant. In addition, there was no significant difference in LAA% and Lm between PBS-treated *Lpcat1* KO and WT mice. H & E staining of lung tissue with PPE treatment also revealed that *Lpcat1* KO mice exhibited more severe emphysema than *Lpcat1* WT mice (Fig. 1b, right column). In contrast, H & E staining of lung tissue after PBS administration did not display any visual difference between *Lpcat1* KO and WT mice (Fig. 1b, left column).

### PPE-Treated *Lpcat1* KO Mice Promoted *Cxcl2*, *Il6*, and *Mmp12* Gene Expression in the Lungs

Subsequently, we examined the cell numbers and cell differentiation in the BALF. PPE administration increased the number of cells in the BALF from 24 h to 7 days. However, the total cell count and the proportion of the cell types in the BALF were not statistically different between WT and *Lpcat1* KO mice (Fig. 2a). To assess cytokine induction following PPE treatment, we examined *Cxcl1*, *Cxcl2*, and *Il6* mRNA expression at similar time points. We selected these cytokines because they have been reported to be upregulated in a ventilator-induced lung injury model of *Lpcat1* KO mice [19] and also because LPCAT1 deficiency has been shown to be involved in the promotion of elastase emphysema [21, 28–30]. Changes in these cytokines were relatively large at 24 h after PPE administration. PPE treatment significantly promoted *Il6* mRNA expression in the whole lung. *Cxcl2* expression tended to be upregulated in KO mice, compared with WT mice, particularly during the early phase after administration (Fig. 2b). In addition, we examined the expression of MMPs and proteases, which are important in





◀ **Fig. 4** CSE stimulation alters the expression of *Lpcat1* in both hAEC2 and A549 cells. (a) Number of genes with altered expression in hAEC2 cells and A549 cells after CSE stimulation. (b) Pathways enriched in CSE-treated hAEC2 cells analyzed by GO analysis. (c) Heat map of genes related to phospholipid biosynthesis in the remodeling pathway (TPM > 0.1), which are present in the 616 genes with altered expression because of CSE administration. CSE: cigarette smoke extract; hAEC2: human type 2 alveolar epithelial cells; GO analysis: gene ontology analysis; TPM: transcripts per kilobase million.

emphysema progression [31]. *Mmp2* and *Mmp12* were upregulated 2 weeks after PPE administration both in WT and KO mice (Fig. 2b). *Mmp2* expression was not different between WT and KO mice. In contrast, *Mmp12* expression was upregulated early after treatment in KO mice compared with that in WT mice, as was *Cxcl2*. Furthermore, we analyzed the PC composition in the BALF. The proportion of DPPC in total PC in *Lpcat1* KO mice was lower than that in WT mice, similar to the results of a previous lipidomic analysis of the BALF [19]. In addition, the DPPC proportion of total phospholipids in the BALF in *Lpcat1* KO mice decreased 1 week after elastase injection, similar to that in WT mice (Fig. 2c, Supplemental Fig. S2).

### DPPC Supplementation Did Not Attenuate the Development of PPE-Induced Emphysema

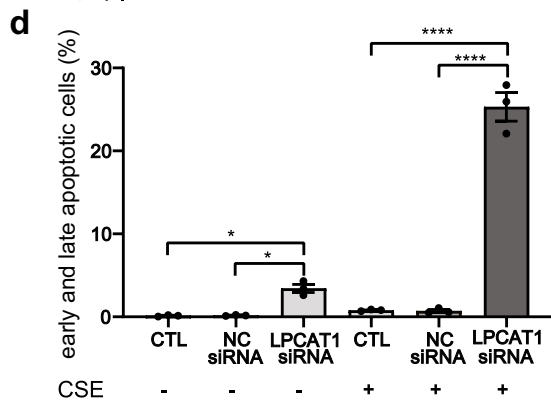
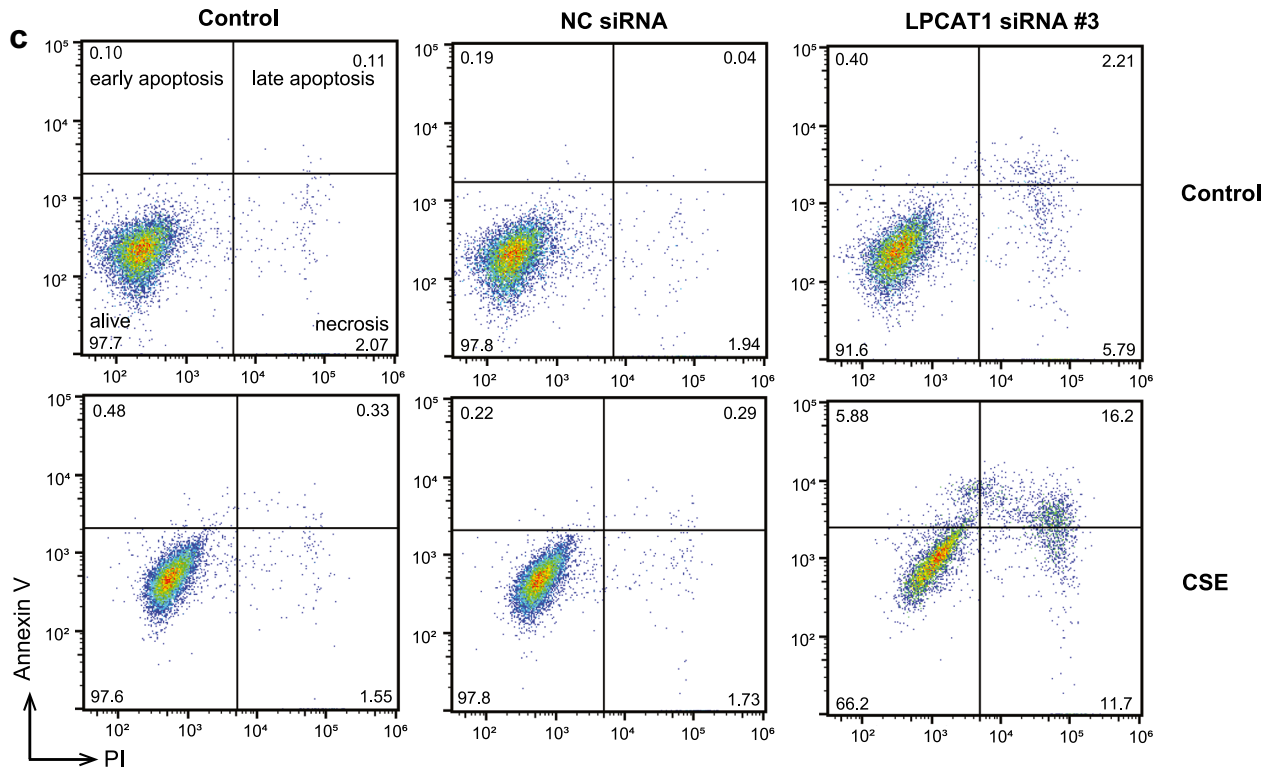
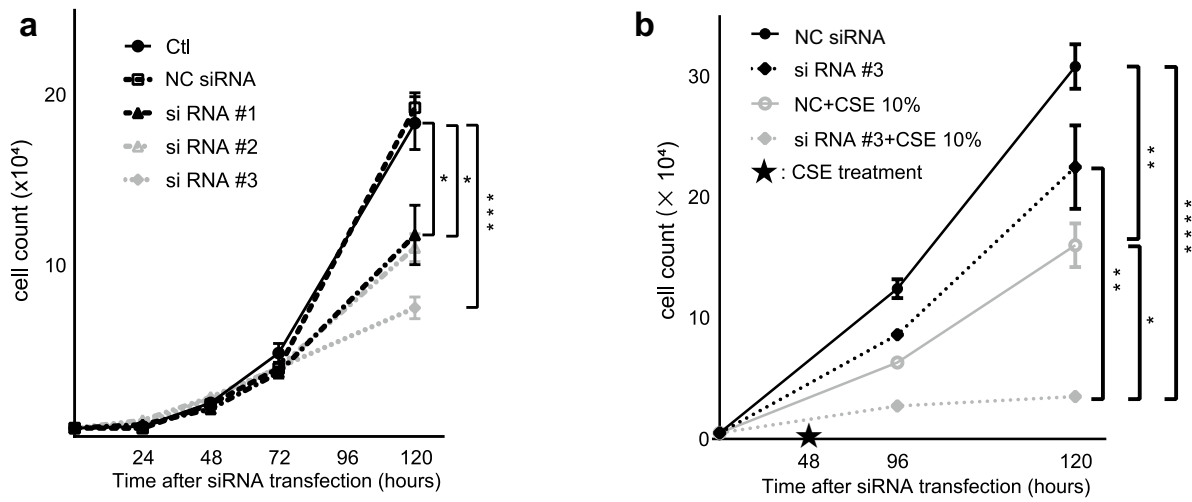
We hypothesized that the lack of LPCAT1 made the PPE-treated mice susceptible to development of lung emphysema through a decrease in DPPC synthesis. Considering that LPCAT1 is a key enzyme for DPPC production and DPPC is the major PC in the surfactant, we administered DPPC to the PPE-treated *Lpcat1* KO mice to determine if artificial surfactant (aSF)–containing DPPC rescued lung emphysema. Palmitoyl-oleoyl-PC, which is not produced by LPCAT1, was used as a control. The lungs of PPE-treated mice were intranasally administered with aSF. We selected intranasal administration since it is a safe and widely used method that has been reported to be comparable with intratracheal administration [32]. We followed two protocols, *i.e.*, aSF was administered before and after treatment with PPE or only after the treatment (Supplemental Fig. S3a, S3c). Contrary to our expectations, neither group revealed improvements in the LAA% and Lm (Supplemental Fig. S3b, S3d).

### *Lpcat1* KO Mice Lungs Displayed Enhanced PPE-Induced Apoptosis

We hypothesized that the enhancement of emphysema in *Lpcat1* KO mice was because of the apoptosis induction in AECs. This can be attributed to the significance of AEC apoptosis in the development of human emphysema [33]. To investigate apoptosis in the lungs following PPE administration, we performed TUNEL staining in *Lpcat1* KO and WT mice at 1 week post-elastase administration (Fig. 3a). Although the PPE-induced inflammation was attenuated within 2 weeks after administration (Fig. 2a and b) and there was no accumulation of inflammatory cells in the lung at 6 weeks after administration, Lm was significantly higher in *Lpcat1* KO mice than that in WT mice (Fig. 1a). We therefore believed that apoptosis commenced soon after PPE administration and remained for 2 weeks. Therefore, we analyzed apoptosis 1 week after PPE administration. PPE-treated *Lpcat1* KO lungs had a relatively higher number of TUNEL-positive (apoptotic) cells than WT lungs (Fig. 3b). Furthermore, *Lpcat1* is specifically expressed in AEC2s, as shown previously [16]. Therefore, we analyzed the number of dead cells in flow cytometry–sorted AEC2s from WT and *Lpcat1* KO mice 1 week after PPE administration. *Lpcat1* KO mice revealed a higher dead cell rate of EpCAM<sup>+</sup> SPC<sup>+</sup> AEC2s in the lung following PPE administration compared with WT mice (Fig. 3c, d). In other words, AEC2s in *Lpcat1* KO mice were more vulnerable to PPE than AEC2s in WT mice.

### *Lpcat1* mRNA Expression Was Altered in Both hAEC2s and A549 Cells with CSE Stimulation

To simulate the *in vivo* situation *in vitro*, we performed a transcriptomic analysis of hAEC2s that were treated with CSE for 48 h and compared them with microarray datasets (GSE77942) [34] from CSE-treated A549 cells, a human alveolar epithelial cell line. A total of 4,705 genes were significantly changed in the CSE-treated hAEC2s, and 616 of them were similar to the significantly changed genes of CSE-treated A549 cells (Fig. 4a). The gene ontology analysis revealed that the CSE-treated cells enriched gene sets related to apoptosis and the regulation of DNA replication (Fig. 4b). CSE treatment downregulated *Lpcat1* expression in hAEC2s. Among the genes related to lysophospholipid



◀ **Fig. 5** *Lpcat1* knockdown increases cell susceptibility to apoptosis. (a) Numbers of cells following *Lpcat1* siRNA transfection. \* $P < 0.05$ , \*\* $P < 0.01$ , and \*\*\* $P < 0.001$  (one-way ANOVA with Tukey's multiple comparisons). (b) Numbers of cells after the addition of CSE for another 48 h after *Lpcat1* knockdown. \* $P < 0.05$ , \*\* $P < 0.01$ , and \*\*\*\* $P < 0.0001$  (two-way ANOVA with Tukey's multiple comparisons). (c) Representative images of flow cytometric analysis using double staining with Annexin V and propidium iodide. The upper left quadrants show the cells in the early apoptotic stage. The upper right quadrants show the cells in the late apoptotic stage. The lower right quadrants show necrotic cells and the lower left quadrants show living cells. (d) The percentage of apoptotic cells (cells in the early and late apoptotic stages; Annexin V–positive cells). Data are presented as mean  $\pm$  standard error of mean ( $n = 3-4$ ). \* $P < 0.05$ , \*\*\*\* $P < 0.0001$  (two-way ANOVA with Tukey's multiple comparisons). siRNA: small interfering RNA; CTL: control; NC siRNA: negative control small interfering RNA; CSE: cigarette smoke extract; PI: propidium iodide; ANOVA: analysis of variance.

acyltransferase, their substrates and biosynthesis [14, 35–38]—which also includes *Lpcat1*—CSE treatment downregulated the expression of *Lpcat3*, *Mboat2*, *Pnpla4*, *Agpat3*, and *Pdah3*. In contrast, CSE treatment upregulated the expression of *Pafah1b2* and *Pnpla8* (Fig. 4c).

### ***Lpcat1* Knockdown Suppressed the Proliferation of A549 Cells and Enhanced CSE-Induced Apoptosis**

LPCAT1 is involved in cell proliferation and apoptosis [39]. We tested the effects of *Lpcat1* knockdown on cell proliferation in A549 cells. *Lpcat1* knockdown significantly reduced cell proliferation (Fig. 5a). CSE significantly attenuated cell proliferation, and the knockdown of *Lpcat1* enhanced the effect of CSE on the cells (Fig. 5b). To confirm the mechanism of the loss of cell proliferation, we performed an apoptosis assay by staining the cells with Annexin V and propidium iodide (PI). The knockdown of *Lpcat1* by small interfering RNA (siRNA) induced both necrotic cells (Annexin V–/PI+) and early and late apoptotic cells (Annexin V+). However, CSE treatment induced moderate apoptosis in WT cells or negative control siRNA-transfected cells (NC siRNA). Moreover, CSE-treated *Lpcat1* knockdown cells revealed higher early and late (Annexin V+) apoptotic cells (Fig. 5c, d). This result indicated that the lack of LPCAT1 increased susceptibility to CSE-induced cell death.

## **DISCUSSION**

We initially hypothesized that LPCAT1 deficiency exacerbated lung emphysema through an imbalance in the proportion of lipids in the alveolar surfactant. To address our hypothesis, we utilized an elastase-induced lung emphysema model for *Lpcat1* KO mice. *Lpcat1* KO mice revealed higher Lm and LAA% than WT mice, which are characteristics of advanced emphysema. However, the addition of artificial surfactants (DPPC, a product of LPCAT1) did not recover emphysema exacerbation. Therefore, we hypothesized that the worsening of lung emphysema because of LPCAT1 deficiency was an outcome of alveolar epithelial apoptosis. Bulk RNA-seq revealed that CSE treatment downregulated lipid synthesis genes in primary hAEC2s. *Lpcat1* siRNA knockdown attenuated the proliferation of lung epithelial cells, and *Lpcat1* knockdown enhanced CSE-induced apoptosis. Therefore, we concluded that LPCAT1 plays an important role in cell survival during the development of lung emphysema.

Previous reports have suggested that LPCAT1 is involved in the synthesis of phospholipids in lung surfactants [19]. LPCAT1 has also been associated with lung diseases, such as the exacerbation of a ventilator lung injury model in *Lpcat1* KO mice [19] and the suppression of oleic acid–induced acute lung injury by *Lpcat1* gene transfer [40]. Our findings revealed that LPCAT1 deficiency exacerbated elastase-induced emphysema (Fig. 1) and elastase reduced DPPC in the BALF (Fig. 2). The percentage of DPPC in the surfactant was decreased in *Lpcat1* KO mice [19] (Fig. 2c); this decrease was shown to reduce the surface tension–lowering effect of the surfactant [19], which may have subsequently weakened the ability to open the alveoli. Therefore, LAA% after PPE administration could be underestimated in the lungs of *Lpcat1* KO mice (Fig. 1a). In addition, bulk RNA-seq data from hAEC2s revealed a significant decrease in the expression of lipid synthesis genes, including *Lpcat1*, following CSE treatment in an *in vitro* model of COPD [41] (Fig. 4). Our findings indicated that the stimulation of tobacco smoke, which is the cause of emphysema, may be involved in emphysema formation through a decrease in LPCAT1, yielding a decrease in DPPC production. In contrast, the supplementation of lung surfactant phospholipids to mice following elastase administration did not improve emphysema (Supplemental Fig. S3). DPPC is a key surfactant lipid in the reduction of surface tension, an

important function of surfactants [19]. A recent study mentioned that DPPC was the most decreased phospholipid in the BALF of *Lpcat1* KO mouse lungs [19]. Nonetheless, changes occur in other phospholipids, such as decrease in palmitoyl-palmitoleoyl-PC and palmitoyl-myristoyl-PC. These PCs can also reduce the surface tension on the alveoli [42]. Furthermore, changes in the proportion of PCs apart from DPPC because of LPCAT1 deficiency (change in surfactant “quality”) may involve the exacerbation of emphysema in *Lpcat1* KO mice. In addition, the intratracheal administration of elastase generally results in more severe emphysematous changes in the lungs than smoking-induced emphysema [43]. The emphysematous changes caused by elastase-induced lung inflammation may be so strong that the supplementation with an artificial surfactant may not be sufficient to reverse these changes (Supplemental Fig. S3). Taken together, we hypothesized that the mechanism of emphysema exacerbation in the lungs of *Lpcat1* KO mice was not limited to changes in LPCAT1-catalyzing surfactant phospholipids.

LPCAT1 is principally expressed in the AEC2s [16]. AEC2s proliferate for alveolar epithelial repair and differentiate into AEC1s in response to lung injury [5, 44]. Previous reports have demonstrated enhanced apoptosis in the alveolar wall in the lungs of patients with emphysema [33]. In addition, AEC2s are senescent in patients with emphysema and have a reduced proliferative capacity [45]. One mouse study suggested that the administration of active caspase-3 protein with Chariot caused emphysema in mice [46]. Our findings suggested that elastase-treated LPCAT1-deficient mice exhibited enhanced apoptosis in the lungs, that AEC2s exhibited a high dead cell rate post-elastase treatment (Fig. 3), and that loss of LPCAT1 in A549 cells promoted apoptosis upon CSE stimulation (Fig. 5). Thus, LPCAT1 deficiency induces AEC2 cell death. We believed that the loss of *Lpcat1* had a long-term effect on this model by inappropriately repairing the lungs through greater damage to the AEC2s involved in lung repair, rather than prolonging short-term inflammation.

LPCAT1 is reportedly upregulated in several carcinomas and is associated with poor prognosis [47] and cancer cell proliferation [48]. Several types of tumors, such as colorectal cancer [49] and renal carcinoma [50], enhance *Lpcat1* expression. These cancer cells promote cell proliferation and alter the lipid composition of the tumor. In addition, an increase in DPPC of the cell membrane because of enhanced *Lpcat1*

expression in glioblastoma increases cell proliferation [51]. This might be due to the positive feedback loop of the LPCAT1 and EGF receptor signaling. Moreover, LPCAT1 reportedly affects the survival of non-cancer cells. The retinal degeneration 11 (*rd11*) mouse model is an animal model with rapid photoreceptor degeneration and carries a mutation in the *Lpcat1* gene [52]. Decreased DPPC levels [52] and increased photoreceptor cell apoptosis [53] have been observed in the *rd11* mouse retina. Reactive oxygen species might be involved in the apoptosis of photoreceptor cells (Shindou H *et al.*, unpublished). In our study, CSE stimulation of AEC2s and A549 cells demonstrated that the *Lpcat1* gene was commonly downregulated and that the commonly upregulated genes in both were associated with apoptosis (Fig. 4). Furthermore, *Lpcat1* siRNA transfection of A549 suppressed cell proliferation and enhanced CSE-stimulated apoptosis (Fig. 5). These findings suggested that LPCAT1 deficiency may contribute to the progression of emphysema by enhancing apoptosis and reducing alveolar repair rather than a change in surfactant production. In addition, CSE stimulation of AEC2s modified the genes involved in phospholipid metabolism, including *Lpcat1*, which necessitates further study.

This study has several limitations. First, the elastase-induced emphysema model used in this study had a different origin compared with human smoking-induced emphysema. However, it is a widely accepted model that can induce emphysema in a short period. Second, the dosage of aSF used in this study may have been too low to improve the elastase-induced emphysema. However, we considered that the dosage and frequency of aSF used in this study corresponded with the limits of safe administration. Third, despite the widespread use of A549 cells as a model for AEC2 biology experiments, they represent a cancer cell line. Considering potential differences among normal AEC2s, we used primary hAEC2s. However, these cells can easily differentiate into AEC1s, and it is difficult to maintain the AEC2 phenotype using conventional culture methods. Recently, Katsura *et al.* reported a novel culture method to maintain the phenotype of AEC2 in organoids without feeder cells [54]. The wide availability of this method would enable its application for further research with respect to AEC2 cell biology.

In conclusion, *Lpcat1* deficiency exacerbated PPE-induced emphysema in mice. Using an *in vitro* COPD model, CSE-treated hAEC2s, we discovered that the expression of numerous lipid synthesis genes

was reduced in these cells, including *Lpcat1*. Eventually, we demonstrated that LPCAT1 deficiency enhanced CSE-induced apoptosis in AEC2s. The protective effects of LPCAT1 on emphysema could be attributed to the inhibition of AEC2 cell apoptosis. The management of LPCAT1 deficiency and lipid alteration by *Lpcat1* gene transfer may be an approach in the future for COPD therapy. Further studies are required to elucidate the mechanism of apoptosis induction by LPCAT1 deficiency-induced lipid changes.

## SUPPLEMENTARY INFORMATION

The online version contains supplementary material available at <https://doi.org/10.1007/s10753-022-01659-4>.

## ACKNOWLEDGEMENTS

We thank Sachika Wada, Chinatsu Yonekawa (Keio University), Miyuki Yamamoto, and Yoshikazu Takahashi (National Center for Global Health and Medicine, NCGM) for their skillful technical assistance.

## AUTHOR CONTRIBUTION

TT, YM, KF, and HS developed the concept and designed the research. TT, YM, TS, TH-Y, SK, and KH performed the experiments and analyzed the data for the work. TT, YM, KF, TS, TH, and HS drafted the manuscript. TT, YM, HS, TS, TH-Y, SK, JM, HK, KM, RH, HK, NM, KM, HM, YS, AM, TM, TN, TS, and KF edited and revised the manuscript. All authors have approved the final version of the manuscript.

## FUNDING

This work was supported by the Japan Society for The Promotion of Science (Grants-in-Aid for Scientific Research, Grant Numbers JP15K19172 and JP18K15945 to YM), GlaxoSmithKline (GSK Japan Research Grant 2016 to YM and GSK Japan Research Grant 2021 to TT), Japan Agency for Medical Research and Development (AMED-CREST, Grant Number JP21gm0919911 to HS), Japan Science and Technology Agency (CREST, Grant Number JPMJCR1689 to RH), and Takeda Science Foundation (Research Grant 2014 and 2017 to TS).

## DECLARATIONS

**Ethical Approval** All animal experiments and procedures were approved by the Laboratory Animal Center, the Keio University School of Medicine (Protocol No. 10258), and were performed in accordance with the institutional guidelines.

**Informed Consent** Informed consent is not applicable in the present study.

**Competing Interests** The authors declare no competing interests.

## REFERENCES

- Vestbo, J., S.S. Hurd, A.G. Agustí, P.W. Jones, C. Vogelmeier, A. Anzueto, P.J. Barnes, L.M. Fabbri, F.J. Martinez, M. Nishimura, R.A. Stockley, D.D. Sin, and R. Rodriguez-Roisin. 2013. Global strategy for the diagnosis, management, and prevention of chronic obstructive pulmonary disease: GOLD executive summary. *American Journal of Respiratory and Critical Care Medicine* 4: 347–365. <https://doi.org/10.1164/rccm.201204-0596PP>.
- Haruna, A., S. Muro, Y. Nakano, T. Ohara, Y. Hoshino, E. Ogawa, T. Hirai, A. Niimi, K. Nishimura, K. Chin, and M. Mishima. 2010. CT scan findings of emphysema predict mortality in COPD. *Chest* 3: 635–640. <https://doi.org/10.1378/chest.09-2836>.
- Crapo, J.D., B.E. Barry, P. Gehr, M. Bachofen, and E.R. Weibel. 1982. Cell number and cell characteristics of the normal human lung. *American Review of Respiratory Disease* 2: 332–337. <https://doi.org/10.1164/arrd.1982.126.2.332>.
- Wynne, B.M., L. Zou, V. Linck, R.S. Hoover, H.P. Ma and D.C. Eaton. 2017. Regulation of lung epithelial sodium channels by cytokines and chemokines. *Frontiers in Immunology* 766. <https://doi.org/10.3389/fimmu.2017.00766>.
- Aspal, M. and R.L. Zemans. 2020. Mechanisms of AIIH-to-ATI cell differentiation during lung regeneration. *International Journal of Molecular Sciences* 9: <https://doi.org/10.3390/ijms21093188>.
- Rangasamy, T., C.Y. Cho, R.K. Thimmulappa, L. Zhen, S.S. Srisuma, T.W. Kensler, M. Yamamoto, I. Petrache, R.M. Tuder, and S. Biswal. 2004. Genetic ablation of Nrf2 enhances susceptibility to cigarette smoke-induced emphysema in mice. *Journal of Clinical Investigation* 9: 1248–1259. <https://doi.org/10.1172/JCI21146>.
- Veldhuizen, R., K. Nag, S. Orgeig, and F. Possmayer. 1998. The role of lipids in pulmonary surfactant. *Biochimica et Biophysica Acta* 2–3: 90–108. [https://doi.org/10.1016/s0925-4439\(98\)00061-1](https://doi.org/10.1016/s0925-4439(98)00061-1).
- Han, S., and R.K. Mallampalli. 2015. The role of surfactant in lung disease and host defense against pulmonary infections. *Annals of the American Thoracic Society* 5: 765–774. <https://doi.org/10.1513/AnnalsATS.201411-507FR>.
- Moré, J. M., D. R. Voelker, L. J. Silveira, M. G. Edwards, E. D. Chan and R. P. Bowler. 2010. Smoking reduces surfactant protein D and phospholipids in patients with and without chronic obstructive pulmonary disease. *BMC Pulmonary Medicine* 53. <https://doi.org/10.1186/1471-2466-10-53>.
- Agudelo, C.W., B.K. Kumley, E. Area-Gomez, Y. Xu, A.J. Dabo, P. Geraghty, M. Campos, R. Foronjy, and I. Garcia-Arcos. 2020. Decreased surfactant lipids correlate with lung function in chronic obstructive pulmonary disease (COPD). *PLoS ONE* 2: e0228279. <https://doi.org/10.1371/journal.pone.0228279>.
- Glasser, S.W., E.A. Detmer, M. Ikegami, C.L. Na, M.T. Stahlman, and J.A. Whitsett. 2003. Pneumonitis and emphysema in sp-C gene targeted mice. *Journal of Biological Chemistry* 16: 14291–14298. <https://doi.org/10.1074/jbc.M210909200>.

12. Wert, S.E., M. Yoshida, A.M. Levine, M. Ikegami, T. Jones, G.F. Ross, J.H. Fisher, T.R. Korfhagen, and J.A. Whitsett. 2000. Increased metalloproteinase activity, oxidant production, and emphysema in surfactant protein D gene-inactivated mice. *Proceedings of the National Academy of Sciences of the United States of America* 11: 5972–5977. <https://doi.org/10.1073/pnas.100448997>.
13. Lands William, E.M. 1958. Metabolism of glycerolipides: a comparison of lecithin and triglyceride synthesis. *Journal of Biological Chemistry* 2: 883–888. [https://doi.org/10.1016/s0021-9258\(18\)70453-5](https://doi.org/10.1016/s0021-9258(18)70453-5).
14. Shindou, H., and T. Shimizu. 2009. Acyl-CoA:lysophospholipid acyltransferases. *Journal of Biological Chemistry* 1: 1–5. <https://doi.org/10.1074/jbc.R800046200>.
15. Valentine, W.J., T. Hashidate-Yoshida, S. Yamamoto and H. Shindou. 2020. Biosynthetic enzymes of membrane glycerophospholipid diversity as therapeutic targets for drug development. *Advances in Experimental Medicine and Biology* 5-27. [https://doi.org/10.1007/978-3-030-50621-6\\_2](https://doi.org/10.1007/978-3-030-50621-6_2).
16. Nakanishi, H., H. Shindou, D. Hishikawa, T. Harayama, R. Ogasawara, A. Suwabe, R. Taguchi, and T. Shimizu. 2006. Cloning and characterization of mouse lung-type acyl-CoA:lysophosphatidylcholine acyltransferase 1 (LPCAT1). Expression in alveolar type II cells and possible involvement in surfactant production. *Journal of Biological Chemistry* 29: 20140–20147. <https://doi.org/10.1074/jbc.M600225200>.
17. Chen, X., B.A. Hyatt, M.L. Mucenski, R.J. Mason, and J.M. Shannon. 2006. Identification and characterization of a lysophosphatidylcholine acyltransferase in alveolar type II cells. *Proceedings of the National Academy of Sciences of the United States of America* 31: 11724–11729. <https://doi.org/10.1073/pnas.0604946103>.
18. Valentine, W.J., K. Yanagida, H. Kawana, N. Kono, N.N. Noda, J. Aoki, and H. Shindou. 2021. Update and nomenclature proposal for mammalian lysophospholipid acyltransferases, which create membrane phospholipid diversity. *Journal of Biological Chemistry* 1: 101470. <https://doi.org/10.1016/j.jbc.2021.101470>.
19. Harayama, T., M. Eto, H. Shindou, Y. Kita, E. Otsubo, D. Hishikawa, S. Ishii, K. Sakimura, M. Mishina, and T. Shimizu. 2014. Lysophospholipid acyltransferases mediate phosphatidylcholine diversification to achieve the physical properties required *in vivo*. *Cell Metabolism* 2: 295–305. <https://doi.org/10.1016/j.cmet.2014.05.019>.
20. Bridges, J.P., M. Ikegami, L.L. Brilli, X. Chen, R.J. Mason, and J.M. Shannon. 2010. LPCAT1 regulates surfactant phospholipid synthesis and is required for transitioning to air breathing in mice. *Journal of Clinical Investigation* 5: 1736–1748. <https://doi.org/10.1172/JCI38061>.
21. Suzuki, S., M. Ishii, T. Asakura, H. Namkoong, S. Okamori, K. Yagi, H. Kamata, T. Kusumoto, S. Kagawa, A.E. Hegab, M. Yoda, K. Horiuchi, N. Hasegawa, and T. Betsuyaku. 2020. ADAM17 protects against elastase-induced emphysema by suppressing CD62L(+) leukocyte infiltration in mice. *American Journal of Physiology: Lung Cellular and Molecular Physiology* 6: L1172–L1182. <https://doi.org/10.1152/ajplung.00214.2019>.
22. Takahashi, S., H. Nakamura, M. Seki, Y. Shiraiishi, M. Yamamoto, M. Furuuchi, T. Nakajima, S. Tsujimura, T. Shirahata, M. Nakamura, N. Minematsu, M. Yamasaki, H. Tatenno, and A. Ishizaka. 2008. Reversal of elastase-induced pulmonary emphysema and promotion of alveolar epithelial cell proliferation by simvastatin in mice. *American Journal of Physiology: Lung Cellular and Molecular Physiology* 5: L882–890. <https://doi.org/10.1152/ajplung.00238.2007>.
23. Sasaki, M., S. Chubachi, N. Kameyama, M. Sato, M. Haraguchi, M. Miyazaki, S. Takahashi, and T. Betsuyaku. 2015. Evaluation of cigarette smoke-induced emphysema in mice using quantitative micro-computed tomography. *American Journal of Physiology: Lung Cellular and Molecular Physiology* 10: L1039–1045. <https://doi.org/10.1152/ajplung.00366.2014>.
24. Artaechevarria, X., D. Blanco, G. De Biurrun, M. Ceresa, D. Perez-Martin, G. Bastarrika, J.P. De Torres, J.J. Zulueta, L.M. Montuenga, C. Ortiz-De-Solorzano, and A. Munoz-Barrutia. 2011. Evaluation of micro-CT for emphysema assessment in mice: comparison with non-radiological techniques. *European Radiology* 5: 954–962. <https://doi.org/10.1007/s00330-010-1982-5>.
25. Hsia, C. C., D. M. Hyde, M. Ochs, E. R. Weibel and Ats Ers Joint Task Force on Quantitative Assessment of Lung Structure. 2010. An official research policy statement of the American Thoracic Society/European Respiratory Society: standards for quantitative assessment of lung structure. *American Journal of Respiratory and Critical Care Medicine* 4: 394–418. <https://doi.org/10.1164/rccm.200809-1522ST>.
26. Asakura, T., M. Ishii, H. Namkoong, S. Suzuki, S. Kagawa, K. Yagi, T. Komiya, T. Hashimoto, S. Okamori, H. Kamata, S. Tasaka, A. Kihara, A.E. Hegab, N. Hasegawa, and T. Betsuyaku. 2018. Sphingosine 1-phosphate receptor modulator ONO-4641 stimulates CD11b(+)Gr-1(+) cell expansion and inhibits lymphocyte infiltration in the lungs to ameliorate murine pulmonary emphysema. *Mucosal Immunology* 6: 1606–1620. <https://doi.org/10.1038/s41385-018-0077-5>.
27. Bligh, E.G., and W.J. Dyer. 1959. A rapid method of total lipid extraction and purification. *Canadian Journal of Biochemistry and Physiology* 8: 911–917. <https://doi.org/10.1139/o59-099>.
28. Takahashi, S., M. Ishii, H. Namkoong, A.E. Hegab, T. Asami, K. Yagi, M. Sasaki, M. Haraguchi, M. Sato, N. Kameyama, T. Asakura, S. Suzuki, S. Tasaka, S. Iwata, N. Hasegawa, and T. Betsuyaku. 2016. Pneumococcal infection aggravates elastase-induced emphysema via matrix metalloproteinase 12 overexpression. *Journal of Infectious Diseases* 6: 1018–1030. <https://doi.org/10.1093/infdis/jiv527>.
29. Plantier, L., S. Marchand-Adam, V.G. Antico Arciuch, L. Boyer, C. De Coster, J. Marchal, R. Bachoual, A. Mailleux, J. Boczkowski, and B. Crestani. 2007. Keratinocyte growth factor protects against elastase-induced pulmonary emphysema in mice. *American Journal of Physiology: Lung Cellular and Molecular Physiology* 5: L1230–L1239. <https://doi.org/10.1152/ajplung.00460.2006>.
30. Tasaka, S., K. Inoue, K. Miyamoto, Y. Nakano, H. Kamata, H. Shinoda, N. Hasegawa, T. Miyasho, M. Satoh, H. Takano, and A. Ishizaka. 2010. Role of interleukin-6 in elastase-induced lung inflammatory changes in mice. *Experimental Lung Research* 6: 362–372. <https://doi.org/10.3109/01902141003678590>.
31. Churg, A., S. Zhou, and J.L. Wright. 2012. Series “matrix metalloproteinases in lung health and disease”: matrix metalloproteinases in COPD. *European Respiratory Journal* 1: 197–209. <https://doi.org/10.1183/09031936.00121611>.
32. Khadangi, F., A.S. Forges, S. Tremblay-Pitre, A. Dufour-Mailhot, C. Henry, M. Boucher, M.J. Beaulieu, M. Morissette, L. Fereydoonad, D. Brunet, A. Robichaud, and Y. Bosse. 2021. Intranasal versus intratracheal exposure to lipopolysaccharides in a murine model of acute respiratory distress syndrome. *Scientific Reports* 1: 7777. <https://doi.org/10.1038/s41598-021-87462-x>.
33. Yokohori, N., K. Aoshiba, and A. Nagai. 2004. Increased levels of cell death and proliferation in alveolar wall cells in patients with pulmonary emphysema. *Chest* 2: 626–632. <https://doi.org/10.1378/chest.125.2.626>.

34. Checa, M., J.S. Hagood, R. Velazquez-Cruz, V. Ruiz, C. García-De-Alba, C. Rangel-Escareño, F. Urrea, C. Becerril, M. Montaña, S. García-Trejo, J. Cisneros Lira, A. Aquino-Gálvez, A. Pardo, and M. Selman. 2016. Cigarette smoke enhances the expression of profibrotic molecules in alveolar epithelial cells. *PLoS ONE* 3: e0150383. <https://doi.org/10.1371/journal.pone.0150383>.
35. Grevengoed, T.J., E.L. Klett and R.A. Coleman. 2014. Acyl-CoA metabolism and partitioning. *Annual Review of Nutrition* 1-30. <https://doi.org/10.1146/annurev-nutr-071813-105541>.
36. Murakami, M., H. Sato and Y. Taketomi. 2020. Updating phospholipase A2 biology. *Biomolecules* 10: <https://doi.org/10.3390/biom10101457>.
37. Quan, J., A.M. Bode and X. Luo. 2021. ACSL family: the regulatory mechanisms and therapeutic implications in cancer. *European Journal of Pharmacology* 174397. <https://doi.org/10.1016/j.ejphar.2021.174397>.
38. Yamashita, A., Y. Hayashi, N. Matsumoto, Y. Nemoto-Sasaki, S. Oka, T. Tanikawa, and T. Sugiura. 2014. Glycerophosphate/acylglycerophosphate acyltransferases. *Biology (Basel)* 4: 801–830. <https://doi.org/10.3390/biology3040801>.
39. Han, C., G. Yu, Y. Mao, S. Song, L. Li, L. Zhou, Z. Wang, Y. Liu, M. Li, and B. Xu. 2020. LPCAT1 enhances castration resistant prostate cancer progression via increased mRNA synthesis and PAF production. *PLoS ONE* 11: e0240801. <https://doi.org/10.1371/journal.pone.0240801>.
40. Zhou, M., K. Osanai, M. Kobayashi, T. Oikawa, K. Nakagawa, S. Mizuno, Y. Muraki, and H. Toga. 2014. Adenovector-mediated gene transfer of lysophosphatidylcholine acyltransferase 1 attenuates oleic acid-induced acute lung injury in rats. *Critical Care Medicine* 11: e716-724. <https://doi.org/10.1097/CCM.0000000000000633>.
41. Krimmer, D.I., and B.G. Oliver. 2011. What can *in vitro* models of COPD tell us? *Pulmonary Pharmacology and Therapeutics* 5: 471–477. <https://doi.org/10.1016/j.pupt.2010.12.002>.
42. Postle, A.D., L.W. Gonzales, W. Bernhard, G.T. Clark, M.H. Godinez, R.I. Godinez, and P.L. Ballard. 2006. Lipidomics of cellular and secreted phospholipids from differentiated human fetal type II alveolar epithelial cells. *Journal of Lipid Research* 6: 1322–1331. <https://doi.org/10.1194/jlr.M600054-JLR200>.
43. Wright, J.L., M. Cosio, and A. Churg. 2008. Animal models of chronic obstructive pulmonary disease. *American Journal of Physiology: Lung Cellular and Molecular Physiology* 1: L1-15. <https://doi.org/10.1152/ajplung.90200.2008>.
44. Barkauskas, C.E., M.J. Crouce, C.R. Rackley, E.J. Bowie, D.R. Keene, B.R. Stripp, S.H. Randell, P.W. Noble, and B.L. Hogan. 2013. Type 2 alveolar cells are stem cells in adult lung. *Journal of Clinical Investigation* 7: 3025–3036. <https://doi.org/10.1172/JCI68782>.
45. Tsuji, T., K. Aoshiba, and A. Nagai. 2006. Alveolar cell senescence in patients with pulmonary emphysema. *American Journal of Respiratory and Critical Care Medicine* 8: 886–893. <https://doi.org/10.1164/rccm.200509-1374OC>.
46. Aoshiba, K., N. Yokohori, and A. Nagai. 2003. Alveolar wall apoptosis causes lung destruction and emphysematous changes. *American Journal of Respiratory Cell and Molecular Biology* 5: 555–562. <https://doi.org/10.1165/rcmb.2002-0090OC>.
47. Lebok, P., A. Von Hassel, J. Meiners, C. Hube-Magg, R. Simon, D. Höflmayer, A. Hinsch, D. Dum, C. Fraune, C. Göbel, K. Möller, G. Sauter, F. Jacobsen, F. Büscheck, K. Prien, T. Krech, R.H. Krech, A. Von Der Assen, L. Wölber, I. Witzel, B. Schmalfeldt, S. Geist, P. Paluchowski, C. Wilke, U. Heilenkötter, L. Terracciano, V. Müller, W. Wilczak and E.C. Burandt. 2019. Up-regulation of lysophosphatidylcholine acyltransferase 1 (LPCAT1) is linked to poor prognosis in breast cancer. *Aging* 18: 7796–7804. <https://doi.org/10.18632/aging.102287>.
48. Wei, C., X. Dong, H. Lu, F. Tong, L. Chen, R. Zhang, J. Dong, Y. Hu, G. Wu, and X. Dong. 2019. LPCAT1 promotes brain metastasis of lung adenocarcinoma by up-regulating PI3K/AKT/MYC pathway. *Journal of Experimental and Clinical Cancer Research* 1: 95. <https://doi.org/10.1186/s13046-019-1092-4>.
49. Mansilla, F., K.A. Da Costa, S. Wang, M. Kruhoffer, T.M. Lewin, T.F. Orntoft, R.A. Coleman, and K. Birkenkamp-Demtroder. 2009. Lysophosphatidylcholine acyltransferase 1 (LPCAT1) overexpression in human colorectal cancer. *Journal of Molecular Medicine (Berlin, Germany)* 1: 85–97. <https://doi.org/10.1007/s00109-008-0409-0>.
50. Du, Y., Q. Wang, X. Zhang, X. Wang, C. Qin, Z. Sheng, H. Yin, C. Jiang, J. Li, and T. Xu. 2017. Lysophosphatidylcholine acyltransferase 1 upregulation and concomitant phospholipid alterations in clear cell renal cell carcinoma. *Journal of Experimental and Clinical Cancer Research* 1: 66. <https://doi.org/10.1186/s13046-017-0525-1>.
51. Bi, J., T.A. Ichu, C. Zanca, H. Yang, W. Zhang, Y. Gu, S. Chowdhry, A. Reed, S. Ikegami, K.M. Turner, W. Zhang, G.R. Villa, S. Wu, O. Quehenberger, W.H. Yong, H.I. Kornblum, J.N. Rich, T.F. Cloughesy, W.K. Cavenee, F.B. Furnari, B.F. Cravatt, and P.S. Mischel. 2019. Oncogene amplification in growth factor signaling pathways renders cancers dependent on membrane lipid remodeling. *Cell Metabolism* 3 (525–538): e528. <https://doi.org/10.1016/j.cmet.2019.06.014>.
52. Friedman, J.S., B. Chang, D.S. Krauth, I. Lopez, N.H. Waseem, R.E. Hurd, K.L. Feathers, K.E. Branham, M. Shaw, G.E. Thomas, M.J. Brooks, C. Liu, H.A. Bakeri, M.M. Campos, C. Maubaret, A.R. Webster, I.R. Rodriguez, D.A. Thompson, S.S. Bhattacharya, R.K. Koenekoop, J.R. Heckenlively, and A. Swaroop. 2010. Loss of lysophosphatidylcholine acyltransferase 1 leads to photoreceptor degeneration in rd11 mice. *Proceedings of the National Academy of Sciences of the United States of America* 35: 15523–15528. <https://doi.org/10.1073/pnas.1002897107>.
53. Zhang, H., X. Li, X. Dai, J. Han, Y. Zhang, Y. Qi, Y. He, Y. Liu, B. Chang and J.J. Pang. 2017. The degeneration and apoptosis patterns of cone photoreceptors in rd11 mice. *Journal of Ophthalmology* 9721362. <https://doi.org/10.1155/2017/9721362>.
54. Katsura, H., V. Sontake, A. Tata, Y. Kobayashi, C.E. Edwards, B.E. Heaton, A. Konkimalla, T. Asakura, Y. Mikami, E.J. Fritch, P.J. Lee, N.S. Heaton, R.C. Boucher, S.H. Randell, R.S. Baric, and P.R. Tata. 2020. Human lung stem cell-based alveolospheres provide insights into SARS-CoV-2-mediated interferon responses and pneumocyte dysfunction. *Cell Stem Cell* 6 (890–904): e898. <https://doi.org/10.1016/j.stem.2020.10.005>.